NBI-99-11

The Transverse Structure of the Baryon Source in Relativistic Heavy Ion Collisions

Alberto Polleri[a, 1], Raffaele Mattiello [a], Igor N. Mishustin[a,b] and Jakob P. Bondorf[a].

[a] *The Niels Bohr Institute, Blegdamsvej 17, DK-2100 Copenhagen Ø, Denmark.*

[b] *The Kurchatov Institute, Russian Scientific Center, Moscow 123182, Russia.*

(6 April 1999)

Abstract

A direct method to reconstruct the transverse structure of the baryon source formed in a relativistic heavy ion collision is presented. The procedure makes use of experimentally measured proton and deuteron spectra and assumes that deuterons are formed via two-nucleon coalescence. The transverse density shape and flow profile are reconstructed for Pb+Pb collisions at the CERN-SPS. The ambiguity with respect to the source temperature is demonstrated and possible ways to resolve it are discussed.

PACS number(s): 25.75 -q, 25.75 -Dw, 25.75.Ld

Keywords: relativistic heavy ion collisions, coalescence model, clusters, transverse flow.

One of the main goals of modern nuclear physics is to understand the behavior of nuclear matter under extreme conditions. This can provide a solid basis for a reliable description of the nuclear equation of state and therefore answer many unsolved problems in astrophysics and early universe cosmology. In laboratory experiments there is only one way towards this goal, which is to study high energy collisions between heavy nuclei.

The complicated non-equilibrium dynamics associated with such collisions are nowadays the object of intensive theoretical investigations. There have been many attempts to develop a realistic approach describing the full space-time evolution of the system [1, 2, 3]. Furthermore, due to the large number of produced particles and their subsequent re-scattering, a certain degree of local thermodynamic equilibrium might be

[1]Present address: Institute for Theoretical Physics, University of Heidelberg, Philosophenweg 19, D-69120 Heidelberg, Germany.

established at an intermediate stage of the reaction [4, 5, 6]. One can therefore try to use simpler models, dealing with the properly parametrised phase space distribution functions for different particle species.

However, on this road one always encounters an inherent problem. What can be measured in an experiment are only the momentum spectra of particles. Each measurement is only a projection of the full phase space information on the space-time points where particles decouple, the so-called freeze-out region. The fundamental ambiguity that several phase space distributions, after summing over the freeze-out coordinates of particles, can lead to the same single particle spectrum is left, in principle, unresolved. We see that one must disentangle what can be referred to as an *inversion problem*.

Although it is clear that independent single particle spectra are not sufficient to resolve the ambiguity, we fortunately have at our disposal a promising probe, the deuteron (light nuclear clusters, in general). Previous studies have shown [7] that deuteron production cross sections can be understood in terms of the phenomenological coalescence model. It is founded on the fact that a neutron and a proton can fuse into a deuteron only if their relative distance in position and momentum space is small, on the order of the size of the deuteron wave function. Furthermore, because of the small binding energy (~ 2 MeV), deuterons can survive break-up only when scatterings are rare. These two constraints reveal that deuteron production can only take place at freeze-out. This is the reason why, with a suitable use of single and composite particle spectra, one can constrain the freeze-out phase space distribution of protons.

Another important observation made in recent experiments [8, 9, 10] is the development of collective effects during the reaction. The collective behavior is revealed by increasing inverse slopes of spectra for particles of increasing mass. This can be understood in terms of collective flow of nuclear matter, leading to a position-dependent local velocity.

In this letter we extend our previous work [11], attempting to reconstruct the phase space distribution of protons directly from the observed proton and deuteron spectra, exploiting the coalescence prescription together with the notion of collective flow. It is assumed that one can characterise the system at freeze out by a position-dependent collective velocity and a position-independent local temperature T_0. We are mainly interested in the transverse dynamics at mid-rapidity for central collisions of large symmetric systems. We therefore make use of a relativistic description of collective flow based on the Bjorken picture for the longitudinal expansion, together with a longitudinally-independent transverse velocity $\vec{v}_\perp(\vec{r}_\perp)$. The contraction of the four-

momentum p^μ with the collective four-velocity u^μ can be written as [12]

$$p_\mu u^\mu(x) = \gamma_\perp(r_\perp)\,(m_\perp \cosh(y-\eta) - \vec{p}_\perp \cdot \vec{v}_\perp(r_\perp))\,, \tag{1}$$

where $m_\perp = \sqrt{m^2 + p_\perp^2}$ is the transverse particle mass while y and η are the momentum and space-time rapidities, respectively. Choosing a transverse profile $n_p(r_\perp)$ for the local density, we can write the proton phase space distribution as

$$f_p(x,p) = (2\pi)^3\, e^{-\,p_\mu u^\mu(x)\,/\,T_0}\, B_p\, n_p(r_\perp)\,. \tag{2}$$

From now on we drop the subscripts in $\gamma_\perp$, $\vec{v}_\perp$ and $\vec{r}_\perp$, understanding that these quantities denote the transverse degrees of freedom. In the above expression the normalisation constant for the Boltzmann factor in the local frame is defined as

$$B_p^{-1} = \int d^3\vec{p}\; e^{-\,m_\perp \cosh y\,/T_0} = 4\pi\, m^2 T_0\, K_2(m/T_0)\,, \tag{3}$$

where K_2 is the modified Bessel function of second order. The local density must be normalised to the measured differential multiplicity dN_p/dy. To do this we first calculate the invariant momentum spectrum. It can be obtained by integrating the phase space distribution on the freeze-out hypersurface, using the Cooper-Frye formula

$$S_p(p_\perp) = \frac{d^3N_p}{dy\, d^2\vec{p}_\perp} = \frac{1}{(2\pi)^3}\int d\sigma_\mu p^\mu\, f_p(x,p)\,. \tag{4}$$

The form of the integration measure follows from our simplifying choice of freeze-out hypersurface as a sheet of constant longitudinal proper time $\tau = \tau_0$. We neglect longitudinal edge effects which are negligible for the mid-rapidity region of the spectra. We also assume a simultaneous freeze-out in the transverse direction and neglect surface emission at $\tau < \tau_0$. Within this assumption the integration measure assumes the form

$$p^\mu d\sigma_\mu = \tau_0\, m_\perp\, cosh(y-\eta)\, d^2\vec{r}\, d\eta\,. \tag{5}$$

After substituting this expression in eq. (4), the η integration can be done analytically. Now the rapidity density can be obtained by integrating out the transverse momentum dependence of $S_p(p_\perp)$. Finally, one arrives at the normalisation condition for the local proton density

$$\frac{dN_p}{dy} = 2\pi\,\tau_0 \int dr\, r\;\gamma(r)\, n_p(r)\,. \tag{6}$$

This completes the definition of the proton phase space distribution.

The deuteron phase space distribution can be calculated on the basis of the coalescence model. In the density matrix formalism [13] one obtains

$$f_d(x,p) = \tfrac{3}{8}\int \frac{d^3\vec{y}\, d^3\vec{q}}{(2\pi)^3}\, f_p(x_+,p_+)\, f_n(x_-,p_-)\, P_d(\vec{y},\vec{q})\,, \tag{7}$$

where the factor $\frac{3}{8}$ accounts for the spin-isospin coupling of the neutron-proton pair into a deuteron state. It is assumed that neutrons (not measured) evolve in the same way as protons and that $f_n = R_{np}\, f_p$, where $R_{np} = 1-1.5$ is the neutron to proton ratio in the source. In the following we will take $R_{np} = 1.2$. The phase space coordinates of the coalescing pair are $x_\pm = x \pm y/2$ and $p_\pm = p/2 \pm q$ while P_d is the Wigner density for the deuteron relative motion. The coalescence prescription is greatly simplified when considering large and hot systems. In this case one can neglect the smearing effect of the deuteron Wigner density in comparison to the characteristic scales of the system in position and momentum space [14]. Then the deuteron phase space distribution becomes

$$f_d(x,p) \simeq \tfrac{3}{8} R_{np} \left[f_p(x, p/2) \right]^2 . \tag{8}$$

This expression simply means that two nucleons, each with 4-momentum $p/2$, form a deuteron with 4-momentum p at space-time point x.

Repeating the same reasoning for deuterons as done above for protons and inserting the corresponding expressions for f_p and f_d into eq. (8), one obtains the relation

$$n_d(r) = \lambda_d \, n_p^2(r) \tag{9}$$

between the local densities of deuterons and protons. The proportionality coefficient λ_d has dimension L^3 and carries information on the characteristic scales in the problem. Its explicit form is

$$\lambda_d = \frac{3}{8} R_{np} (2\pi)^3 \frac{B_p^2}{B_d} . \tag{10}$$

We now have built up the framework to establish the reconstruction procedure. In a fashion which holds both for protons and for deuterons, using eqs. (2), (4) and (5), we can calculate their invariant momentum spectra. Due to our simple choice of freeze-out hypersurface the integrations over the space-time rapidity and the azimuthal angle can be easily performed, leading to the expression [4]

$$S(p_\perp) = C \int dr\, r\, K_1\!\left(\frac{\gamma(r) m_\perp}{T_0}\right) I_0\!\left(\frac{v(r)\gamma(r) p_\perp}{T_0}\right) \tau_0 n(r), \tag{11}$$

where $C = 4\pi\, B\, m_\perp$ and K_1 and I_0 are modified Bessel functions of first and zeroth order. Here one can explicitly see the ambiguity in the description of the individual single particle spectrum. The two functions $v(r)$ and $n(r)$ cannot be mapped out uniquely from only one function as with the transverse momentum spectrum. This is true if protons and deuterons are treated independently, but with the link provided by the coalescence model, this ambiguity can, at least partially, be removed. Let us

introduce for convenience a new, dimensionless, density function

$$\tilde{n}(v) = \frac{r\,dr}{v\,dv}\,\tau_0\,n(r) \tag{12}$$

and change the integration variable in eq. (11) from r to v. In this way we obtain the new expression for the momentum spectrum

$$S(p_\perp) = C\int dv v\,K_1(\frac{\gamma\,m_\perp}{T_0})\,I_0(\frac{v\,\gamma\,p_\perp}{T_0})\,\tilde{n}(v)\,, \tag{13}$$

from which the one-to-one correspondence between $\tilde{n}(v)$ and $S(p_\perp)$ is evident, since all the functions in the integrand are single-valued. The normalisation condition (6) for $n_p(r)$, due to the definition (12), now becomes

$$\frac{dN_p}{dy} = 2\pi\int dv\,v\;\gamma\;\tilde{n}_p(v)\,, \tag{14}$$

together with the analogous one for $\tilde{n}_d$. It is instructive to consider the limit $T_0 \to 0$ in eq. (13). Using the asymptotic expression for large argument for the Bessel functions K_1 and I_0 and performing the integration with the saddle point method, one obtains that $v = p_\perp/m_\perp$ and $m_\perp = m\gamma$. The transverse momentum spectrum is simply expressed through $\tilde{n}$ as

$$S(p_\perp) \sim \frac{m}{m_\perp^3}\,\tilde{n}(p_\perp/m_\perp)\,. \tag{15}$$

One can easily find $\tilde{n}$ when the observed spectrum has an exponential shape with inverse slope T_* as

$$S^{exp}(p_\perp) \sim \frac{m_\perp}{(m\,T_*)^{3/2}}e^{-(m_\perp - m)/T_*}\,. \tag{16}$$

Expressing the momentum variable in terms of velocity, $p_\perp = mv\gamma$, we obtain

$$\tilde{n}(v) \sim \gamma^4\,b_0^{3/2}e^{-\,b_0\,(\gamma-1)}\,, \tag{17}$$

with $b_0 = m/T_*$. Observe that the exponent behaves as $\exp(-\,b_0\,v^2/2)$ for small v and as $\exp(-\,b_0\,\gamma)$ for large v. In the limiting case $T_0 \to 0$ the function $\tilde{n}$ is therefore uniquely determined from the spectrum. A finite temperature introduces an inevitable intrinsic smearing, which precludes an exact determination of $\tilde{n}$ for a single particle species.

The role of the coalescence model is now to establish the link between proton and deuteron spectra. Substituting in eq. (9) the definition of $\tilde{n}$ from eq. (12), both for protons and for deuterons, we obtain the simple differential equation

$$\tilde{n}_d(v) = \frac{\lambda_d}{\tau_0}\,\frac{v\,dv}{r\,dr}\;\tilde{n}_p^2(v)\,, \tag{18}$$

which can be directly integrated and leads to the closed solution

$$r^2 = 2\,\frac{\lambda_d}{\tau_0}\int_0^v du\,u\,\frac{\tilde{n}_p^2(u)}{\tilde{n}_d(u)}\,. \tag{19}$$

Therefore, by independently extracting the functions $\tilde{n}_p$ and $\tilde{n}_d$ from the observed momentum spectra $S_p(p_\perp)$ and $S_d(p_\perp)$, we can find the function $r(v)$ by a simple numerical integration. Inverting the obtained function as $r(v) \to v(r)$, we obtain the collective velocity profile. Substituting it in eq. (12), we finally obtain the local proton density

$$n_p(r) = \frac{v(r)}{r}\;\frac{dv(r)}{dr}\;\frac{\tilde{n}_p(v(r))}{\tau_0}\,. \tag{20}$$

We now explore more closely the content of eqs. (19) and (20). Taking the limit for small transverse velocity in eq. (19), one finds that $v(r) \simeq H\,r$ and the dimensionful scale in position space is set by the "Hubble constant"

$$H = \left(\frac{\tau_0\,\tilde{n}_d(0)}{\lambda_d\,\tilde{n}_p^2(0)}\right)^{1/2} = \left(\frac{\tau_0}{3\,R_{np}}\left(\frac{m\,T_0}{\pi}\right)^{3/2}\frac{\tilde{n}_d(0)}{\tilde{n}_p^2(0)}\right)^{1/2}. \tag{21}$$

The r.h.s. of this expression is obtained from eqs. (3) and (10), using the asymptotic expression for large argument for the Bessel function K_2 in the Boltzmann factors. Using this result and taking the limit for $r \to 0$ in eq. (20), we obtain the proton spatial density at the origin

$$n_p(0) \simeq \frac{1}{3\,R_{np}}\left(\frac{m\,T_0}{\pi}\right)^{3/2}\frac{\tilde{n}_d(0)}{\tilde{n}_p(0)}\,. \tag{22}$$

This result will be used in the following discussion.

The described procedure to reconstruct the proton phase space distribution can now be applied to the transverse momentum spectra, measured by the NA44 collaboration at the CERN-SPS, for Pb+Pb collisions at 158 A GeV [15]. Using these data, we fitted $\tilde{n}_p$ and $\tilde{n}_d$, using eq. (13) for protons and deuterons and assuming different values for T_0. Guided by eq. (17) we chose a rather flexible form of the profile function, characterized by three parameters, k, a and b, as

$$\tilde{n}(v) \sim \gamma^k\,e^{-(a-b/2)\,v^2-b\,(\gamma-1)}\,. \tag{23}$$

The exponential factor has now the limiting behavior $\exp(-a\,v^2)$ for small v, while $\exp(-b\,\gamma)$ for large v. We separated the scales a and b for small and large v, in order to have more freedom in fitting the curvature of the spectrum. The parameters k_p,

a_p, b_p, k_d, a_d, b_d, are extracted from the experimental data with a Monte Carlo search minimising

$$\chi^2 = \sum_j \left(\frac{S^{exp}(p_j) - S^{theo}(p_j)}{S^{exp}(p_j)} \right)^2 . \tag{24}$$

The only constraint imposed was $\delta_d > 2\delta_p$: because of our choice of $\tilde{n}$ in eq. (23), the integrand in eq. (19) is exponentially divergent for $v \to 1$, thereby giving the limit $v(r) \to 1$ for $r \to \infty$. The values obtained in this way are listed in Tab. 1 and the reconstructed function $\tilde{n}_p$ is shown in Fig. 1. We do not show the deuteron profile since it is very similar to the proton one. The fitted spectra, normalised as $dN_p/dy = 22$ and $dN_d/dy = 0.3$, are shown in Fig. 2. One clearly sees that the calculated spectra for different temperatures are indistinguishable from one another. On the other hand, the reconstructed profiles $\tilde{n}$ are very different for different temperatures. They are very much peaked at large temperatures and become broad as the temperature drops. This is simple to understand, since a lower temperature introduces less momentum spread than a higher one and $\tilde{n}$ compensates for that by broadening. One can notice that the high-temperature profiles have a structure resembling a blast wave [16] where most particles have approximately the same velocity.

In all calculations the freeze-out time was fixed at $\tau_0 = 10$ fm/c [17]. After numerical integration of eq. (19), we obtained the function $v(r)$ shown in Fig. 3 for different temperatures. It shows a linear rise at small r and saturates for large r. The velocity profiles clearly depend on the temperature chosen.

Making use of eq. (20) we also obtained the local proton density, plotted in Fig. 4. One can observe a behavior similar to $\tilde{n}_p$. At high temperature the density shows a shell-like structure which disappears as the temperature is lower. It should be emphasised that the shapes of $v(r)$ and $n_p(r)$ are quite sensitive to the curvature of the momentum spectra.

From the plots of $v(r)$ in Fig. 3, one might have the impression that flow is somehow stronger at high temperature. This is not the case, since the apparent flattening of $v(r)$ at small r is accompanied by a higher saturation value and a corresponding larger extension of $n_p(r)$. To see this more quantitatively we calculated the mean-square value for the velocity field. The mean, taken with respect to the proton density in the global frame defined by $\rho_p(r) = \gamma(r)\, n_p(r)$, is calculated as

$$\langle\, v^2 \,\rangle = \left(\frac{dN_p}{dy} \right)^{-1} \int d^2r \; v^2(r) \; \tau_0 \, \rho_p(r) \,, \tag{25}$$

and the results are listed in Tab. 1 for different temperatures. As one can see, $\langle\, v^2 \,\rangle^{1/2}$ indeed grows with decreasing T_0.

The broadening of n_p as the temperature decreases is dictated by the conservation of the total phase space volume. The particular value chosen for τ_0 also affects the resulting transverse extension of the source. All of this is evident after examining eq. (21). A large temperature results in a large H, *i.e.* in a smaller transverse extension scale H^{-1}. As a consequence the average proton density is larger. This is explicit in eq. (22). To quantify the transverse size of the source we have also calculated the mean-square transverse radius

$$\langle\, r^2 \,\rangle = \left(\frac{dN_p}{dy}\right)^{-1} \int d^2r \; r^2 \; \tau_0 \, \rho_p(r) \,. \tag{26}$$

The resulting values of $\langle\, r^2 \,\rangle^{1/2}$ are listed in Tab. 1. One can observe the increasing mean transverse size with decreasing temperature. It is therefore necessary to know T_0 precisely in order to determine the system size. This information cannot be extracted solely from proton and deuteron spectra. Contrary to what is commonly done, source radii *cannot* be extracted from the d/p^2 ratio (usually assumed to be inversely proportional to the source volume) unless T_0 is known or further assumptions are made. One possibility relies on a rough estimate of the characteristic value of n_p at freeze-out. Taking the total hadron number density to be $\sim \rho_0/3$, where $\rho_0 = 0.17$ fm^{-3} is the nuclear saturation density, with an average hadron-hadron cross section of ~ 30 mb, we have a mean free path of ~ 6 fm. This is long enough to reach the freeze-out conditions, especially for a rapidly expanding system. Since the ratio of all hadrons (p, n, π, K, ...) to protons is ~ 15 for Pb+Pb collisions at 158 A GeV [18], we can estimate that

$$n_p \simeq \frac{1}{15} \times \frac{1}{3} \times 0.17 \text{ fm}^{-3} \simeq 0.0038 \text{ fm}^{-3} \,. \tag{27}$$

With this number, one can say that our reconstruction procedure suggests the preferred values of $T_0 \simeq 100$ MeV and $\langle\, r^2 \,\rangle^{1/2} \simeq 9.2$ fm, as follows from Fig. 4 and Tab. 1. This is also consistent with the temperature dependence in eq. (22). Comparison with microscopic simulations of the freeze-out distributions at AGS energies [19, 20] and at SPS energies [21] also shows that the temperature around 100 MeV would be preferable. To make a definite statement, one must finally keep in mind that the average source size is influenced by the choice of τ_0. A larger (smaller) value would result in a smaller (larger) average size. Internal consistency requires that τ_0 is large enough so that the flow field has time to develop and the source to expand transversely during the reaction. Details about these isuues can only be discussed within a dynamical calculation, unless an independent measurement of τ_0 is available.

It is clear that to resolve the remaining ambiguity in the source temperature one needs some additional experimental information. Recently, $\pi\,\pi$ HBT correlations data

were used as a constraint [22]. Since pions may freeze-out in a different way than protons, it would be even better to consider $p\,p$ HBT correlations, although they are much more sensitive to final state interactions than pions. We would also like to mention that the neutron phase space distribution, here assumed to be proportional to the proton one, could be also reconstructed with a similar procedure for triton spectra. Furthermore, heavier clusters are more sensitive to collective flow than to temperature [20], providing additional constraints.

In conclusion, we have demonstrated how the proton phase space distribution at freeze-out can be reconstructed from the measured transverse momentum spectra of protons and deuterons. The calculations, made with several simplifying assumptions, show that the proposed method gives meaningful results, although the ambiguity with respect to the temperature of the source remains. Two modifications will make this approach more realistic. First, the deuteron size should be explicitly included in the calculation. The wave function's tail plays a quantitatively important role, especially at high energies, when the large number of produced particles forces nucleons to be far apart at freeze-out. Second, the freeze-out hypersurface itself is more complicated than a constant proper time hyperbola. A correct description of early evaporation of fast particles is needed in order to have the high momentum part of the spectra under control. Nevertheless the described procedure provides a basis for more quantitative analyses, possibly including HBT correlations for protons.

The authors would like to thank Andrew Jackson for many valuable and constructive suggestions and Ian Bearden, Jens Jørgen Gaardøje, Allan Hansen and the NA44 group for a very fruitful collaboration and for providing their preliminary data for our analysis. This work was supported in part by I.N.F.N. (Italy).

References

[1] H. Sorge, Phys. Rev. **C52**, 3291 (1995)

[2] K. Geiger, Comput. Phys. Commun. **104**, 70 (1997)

[3] S.A. Bass *et al.*, Prog. Part. Nucl. Phys. **41**, 225 (1998).

[4] E. Schnedermann, J. Sollfrank and U. Heinz, Phys. Rev. C **48**, 2462 (1993).

[5] P. Braun-Munzinger, J. Stachel, J.P. Wessels and N. Xu, Phys. Lett. **B344**, 43 (1995); **B365**, 1 (1996)

[6] J. Cleymans, D. Elliott, H. Satz and R.L. Thews, Z. Phys. **C74**, 319 (1997)

[7] L.P. Csernai and J.I. Kapusta, Phys. Rep. **131**, 223 (1986).

[8] T. Abbott *et al.*, E802 Collaboration, Phys. Rev. C **50**, 1024 (1994).

[9] I. Bearden *et al.*, NA44 Collaboration, Phys. Rev. Lett. **78**, 2080 (1997).

[10] W. Reisdorf *et al.*, FOPI Collaboration, Nucl. Phys. A **612**, 493 (1997).

[11] A. Polleri, J.P. Bondorf and I.N. Mishustin, Phys. Lett. B **419**, 19 (1998).

[12] P.V. Ruuskanen, Acta Phys. Pol. B **18**, 551 (1987).

[13] H. Sato and K. Yazaki, Phys. Lett. B **98**, 153 (1981).

[14] R. Bond, P.J. Johansen, S.E. Koonin and S. Garpman, Phys. Lett. B **71**, 43 (1977).

[15] I. Bearden *et al.*, NA44 Collaboration, *private communication*.

[16] P.J. Siemens and J.O Rasmussen, Phys. Rev. Lett. **42** 880 (1979).

[17] H.W. Barz, J.P. Bondorf, J.J. Gaardhoje and H. Heiselberg, Phys. Rev. **C56**, 1553 (1997)

[18] H. Appelshäuser *et al.*, Nucl. Phys. A **638**, 91c (1998).

[19] L.V. Bravina, I.N. Mishustin, N.S. Amelin, J.P. Bondorf and L.P. Csernai, Phys. Lett. **B354**, 196 (1995); Heavy Ion Phys. **5** 455 (1997).

[20] R. Mattiello *et al.*, Phys. Rev. Lett. **74**, 2180 (1995); R. Mattiello, H. Sorge, H. Stöcker and W. Greiner, Phys. Rev. C **55**, 1443 (1997).

[21] H. Sorge, Phys. Lett. **B373**, 116 (1996).

[22] R. Scheibl and U. Heinz, Phys. Rev. **C59**, 1585 (1998).

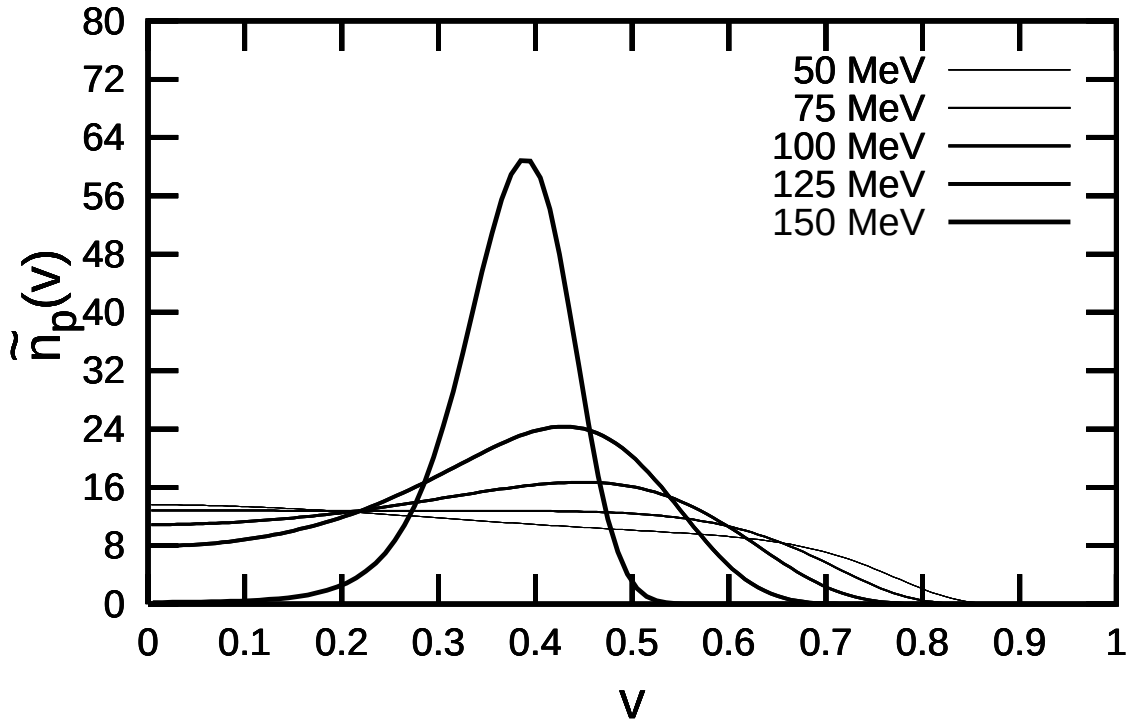

Figure 1: Profile $\tilde{n}_p$, characterized by the parameters shown in tab. 1.

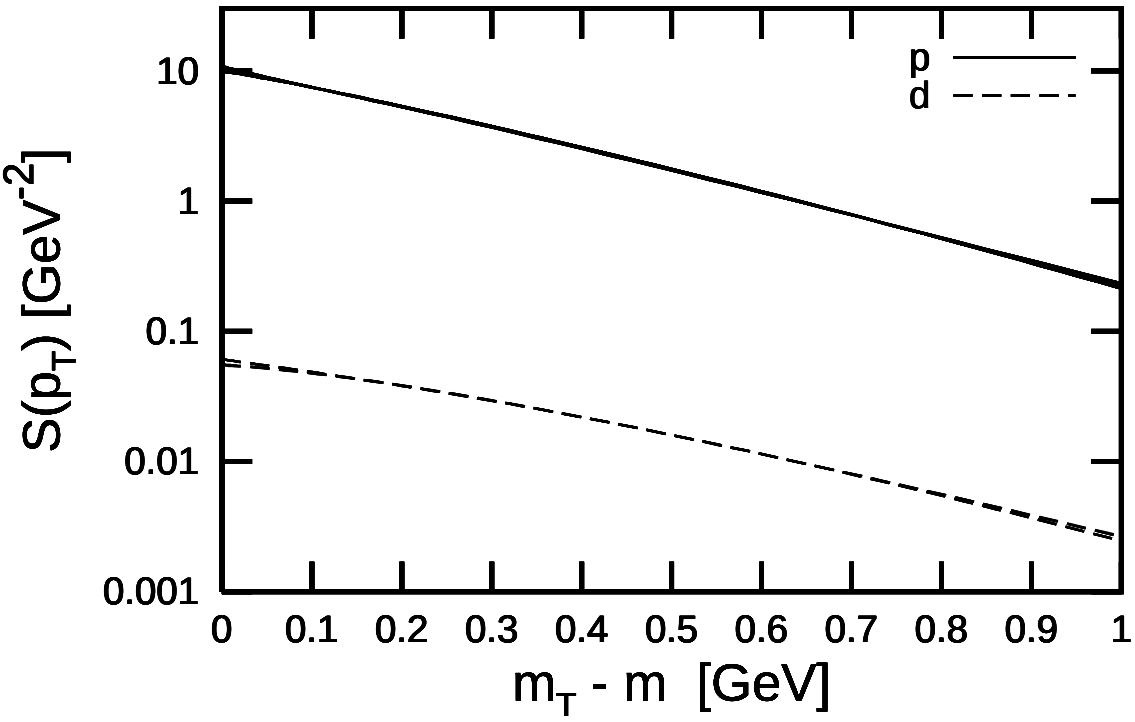

Figure 2: Transverse momentum spectra for protons (top) and deuterons (bottom), plotted as functions of $m_\perp - m$. They are obtained by fitting the NA44 data [15], using the trial functions of eq. (13) with the parameters shown in Tab. 1. Calculated curves corresponding to different temperatures are superimposed and indistinguishable.

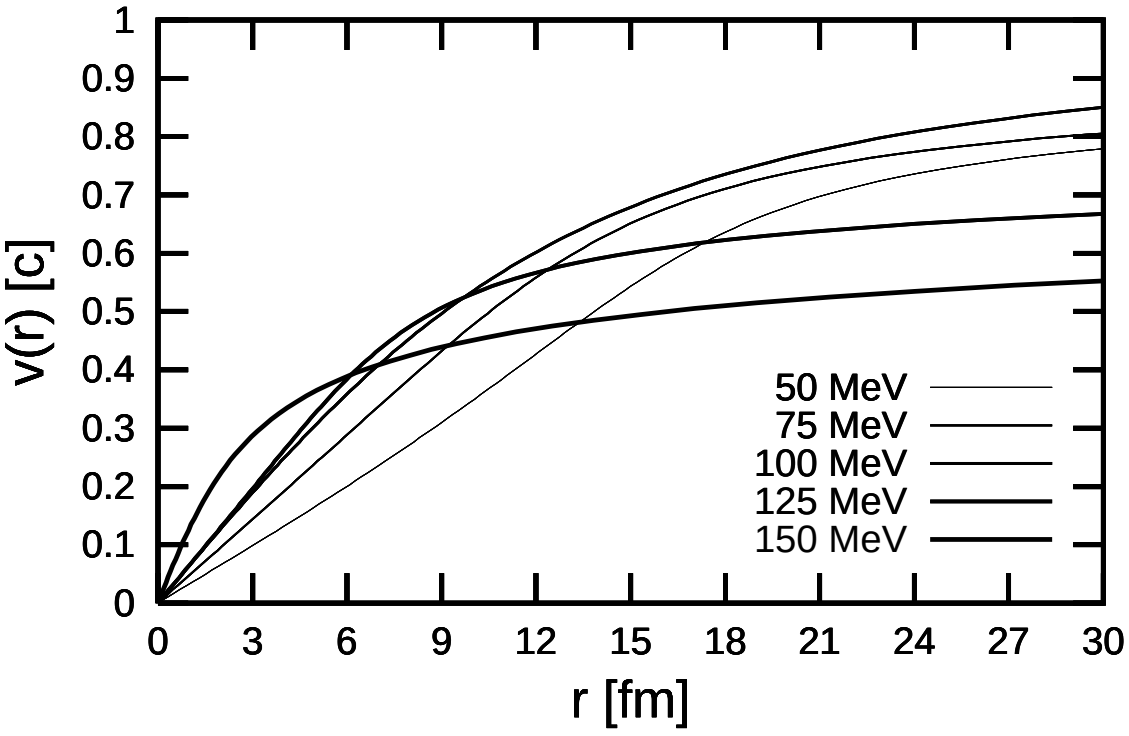

Figure 3: Reconstructed transverse flow velocity fields for different temperatures. The profiles shows a strong rise at small r, levelling off at large r.

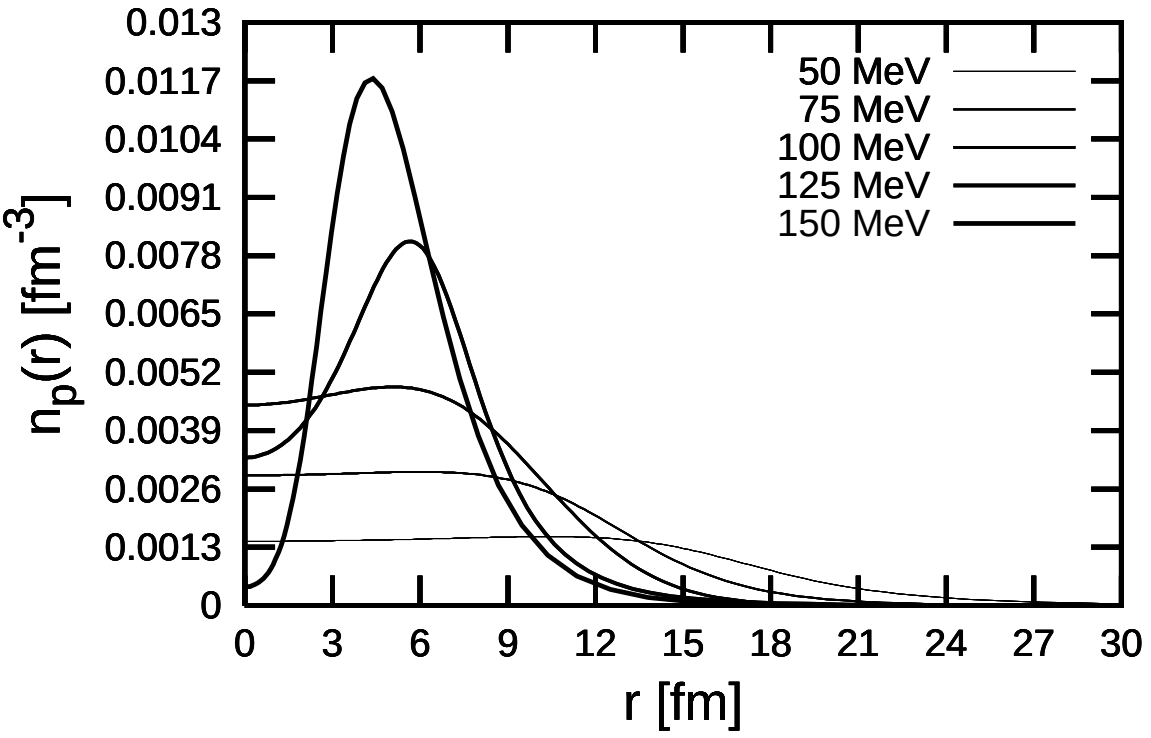

Figure 4: Reconstructed local density of protons as a function of the transverse coordinate. The resulting profile shows a shell-like structure at high temperature, turning into a more uniform behavior at smaller T_0.

Table 1: Fitted parameters characterizing the profiles $\tilde{n}_p$ and $\tilde{n}_d$ for different values of the source temperature T_0. Root-mean-square values for velocity and transverse radius are also listed.

T_0 (MeV)	k_p / k_d	a_p / a_d	b_p / b_d	$\langle v^2 \rangle^{1/2}$	$\langle r^2 \rangle^{1/2}$ (fm)
50	91.56	47.63	52.40	0.54	17.60
	165.29	83.55	107.77		
75	108.50	54.37	68.91	0.51	11.93
	214.21	106.65	146.04		
100	75.86	34.19	66.45	0.48	9.20
	146.62	67.85	133.62		
125	68.48	23.18	105.00	0.44	8.49
	67.24	9.78	211.05		
150	172.89	17.47	602.83	0.39	7.02
	307.96	31.06	1211.85		